JOURNAL OF AIRCRAFT
Vol. 47, No. 5, September–October 2010

Optimization and Postbuckling Analysis of Curvilinear-Stiffened Panels Under Multiple-Load Cases

Thi D. Dang,* Rakesh K. Kapania,† Wesley C. H. Slemp,‡ Manav Bhatia,§ and Sham P. Gurav¶
Virginia Polytechnic Institute and State University, Blacksburg, Virginia 24061

DOI: 10.2514/1.C000249

Recent studies have indicated that panels with curvilinear stiffeners offer a strong potential for structural tailoring. However, the design complexity requires use of numerical analysis and optimization techniques. This paper considers the problem of optimal design of a stiffened panel with cutouts and curvilinear stiffeners, under multiple-load cases. Multiple failure modes are considered: buckling, damage tolerance, stress, and crippling. An optimization framework is presented to minimize mass of the stiffened panel by a combined shape and sizing optimization subject to constraints on the individual failure modes. Different panel thicknesses are allowed for each region bounded by stiffeners or panel boundaries. The framework uses Python scripts to couple ABAQUS-based analysis with VisualDoc optimization package. A design example is presented to illustrate the capability, and the optimized design is compared with that obtained using industry-standard practices. A postbuckling analysis of the optimal design with four curvilinear stiffeners is carried out and discussed in detail.

I. Introduction

THE entire range of engineering disciplines, be it aerospace, ocean, civil, mechanical, electrical, etc., agree on two fundamental needs: lower total costs of the systems being built and maintained, and the ability to tune performance for specific needs. Both of these can be achieved through optimization of individual subsystems, but often, when the performance requirements start to push on individual subsystem boundaries, multidisciplinary interactions become nonnegligible. Hence, any realizable performance improvements and cost reductions have to be based on sound multidisciplinary analysis and optimization.

In aerospace engineering, the notion of structural tailoring is now well established. Composite materials allow the structural designers to provide directional stiffness, thereby providing greater freedom to tailor system behavior at the material level, which is exploited at a larger structural scale. For example, the wing skin can be made of a specific layup of composite fibers to achieve the desired bending-torsion or extension-bending-torsion coupling of the wing deformation. Metals, on the other hand, are generally isotropic in nature, and do not allow for any tailoring at the material level. Hence, the freedom available to tailor metallic structures has been far less in comparison with composites. Although this could be achieved through use of curved spars, ribs or stiffeners, manufacturing difficulties have significantly limited this aspect. Still, metals have an undisputable advantage since their failure models are thoroughly well understood.

Metallic built-up structures have traditionally been created using fasteners, which have well known problems of reduced strength (in comparison with unit metal structure built without fasteners), fatigue, damage tolerance, and high assembly time and maintenance. Recent advances in manufacturing processing, such as high-speed machining, friction-stir welding, etc., have helped in circumventing many of these problems by enabling processes to build larger structural components with complicated shapes at lower associated costs and time. For instance, Boeing [1] developed an integrally-stiffened fuselage concept whose analyses and experimental tests demonstrated equal or better performance than conventional designs with regard to weight and structural integrity, while achieving a significant reduction in manufacturing cost. Recent developments such as friction-stir welding [2] and electron beam freeform fabrication, EBF^3 [3] have shown a strong potential to increase this advantage of unitized structures (see Fig. 1) through additive manufacturing, as opposed to subtractive manufacturing (such as machining).

The benefits of unitized structures [4] can be summarized as a) reduce part count, manufacturing cycle time, and fabrication cost; b) added design flexibility, weight savings, inspectability, and resistance to fatigue and corrosion; c) enhanced automation, improved ergonomics and reduced work fatigue and corrosion; and d) increased determinant assembly opportunities, improve fit and reduce rework. Experts also pointed out that the use of unitized structure is expected to grow exponentially by the year 2020 [5]. With the availability of such advanced manufacturing capabilities, the challenge is now to create a design environment that can exploit these possibilities. The current research aims to exploit this manufacturing advantage through use of multidisciplinary design optimization to design stiffened structures with curved-stiffener geometries. As shown in our recent studies that the stiffeners in the optimized design turned out to be curvilinear rather than straight for some shear dominant load cases, thus exploiting their potential use in the case of panels under shear dominated loadings. And the use of the curvilinear stiffeners in the optimal design is effective in significantly reducing the von Mises stress and increasing the critical buckling load of unitized structures [6]. Moreover, it was shown that the curvilinear stiffeners are more flexible in arresting cracks or damages and thus could help prolong the life of the panel under fatigue failure [7]. Because curvilinear stiffeners are more flexible than straight stiffeners, they are useful for complex panels with cutouts under complex loadings such as the biaxial compression or tension loading combining with the transverse/shear loadings. Therefore, the goal of the use of curvilinear stiffeners is obviously to be weight savings.

An optimization framework is develop for design of a stiffened panel under multiple-load cases and multiple failure modes of buckling, damage tolerance, maximum yield stress and maximum crippling stress in stiffeners. The specific panels considered in the

Presented as Paper 2009-2550 at the 50th AIAA/ASME/ASCE/AHS/ASC Structures, Structural Dynamics, and Materials Conference, Palm Springs, CA, 4–7 May 2009; received 7 January 2010; revision received 16 April 2010; accepted for publication 14 May 2010.

*Postdoctoral Research Associate, Department of Aerospace and Ocean Engineering; ddthi@vt.edu. Member AIAA.

†Mitchell Professor, Department of Aerospace and Ocean Engineering; rkapania@vt.edu. Associate Fellow AIAA.

‡Ph.D. Student, Department of Aerospace and Ocean Engineering; currently with Orbital Mechanics; wslemp@vt.edu.

§Postdoctoral Research Associate, Department of Aerospace and Ocean Engineering; manav@vt.edu. Senior Member AIAA.

¶Former Postdoctoral Research Associate, Department of Aerospace and Ocean Engineering; sham@vt.edu. Member AIAA.

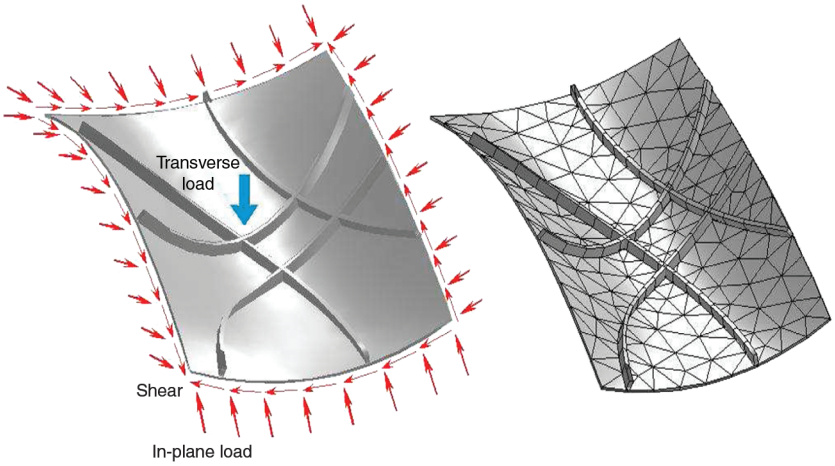

Fig. 1 Unitized structure: stiffened panel with curvilinear stiffeners.

present work have ring-stiffened cutouts, which makes it important to consider both damage tolerance and buckling failure modes. This is due to the fact that a cutout leads to local stress concentration around the hole, and the changes in stress distribution can lead to localized buckling even when the panel is under tensile loads [8]. The framework is based on the environment, EBF3PanelOpt [6,7] that was developed as a part of the ongoing studies on design optimization of curvilinear-stiffened panels. The framework uses Python scripts to couple ABAQUS-based analysis and VisualDoc [9] optimization package. Further details of this framework and optimization problem are presented in later sections.

The framework is used to design two separate panels, one with two stiffeners and one hole, and the other with four stiffeners and two holes. In preparation for testing the four-stiffener panel in NASA Langley's combined compression-shear load fixture [10], a detailed postbuckling analysis of the four-stiffener panel is performed and the results are discussed in this paper.

Section II of the paper presents details of the optimization framework and states the optimization problem. The details of the parametric geometry model generation and response evaluation are presented. Design examples and the optimization results are presented in Sec. III. The optimal design is compared with that obtained from a separate industry-standard procedure, some discussions are also given in this section. The postbuckling analysis of the four-stiffener design is presented in Sec. IV. Finally, conclusions are summarized in Sec. V.

II. Optimization Problem and Framework

A. Framework Development for Optimization Problem

A previous study by Dang et al. [7] presented sizing optimization of stiffened panel with damage tolerance constraint, and a crack propagation study on the optimized panel. An initial flaw was assumed to be present at the location of maximum stress and its propagation path was predicted. The stress intensity factor K was evaluated during the course of this propagation, and it was shown that the stiffeners could help prolong the life of the panel under fatigue load. In the present work, a similar procedure is followed for calculation and of the stress and intensity factor, K. However, the framework is enhanced to account for four stiffeners and panels cutouts.

In the current framework the constraints are based on static stress, buckling and damage tolerance analysis. These analyses are performed using ABAQUS. The Python programming environment is used to interface and enable data exchange between various units of ABAQUS (see Fig. 2), this is because ABAQUS has a Python-based application programming interface for connecting ABAQUS to other codes, which can be effectively leveraged to automate various subtask for analysis and design. The parametric design and finite element mesh are created using the ABAQUS computer aided environment (CAE) preprocessor, which provides the model input file. This file is then adapted for boundary conditions of each load case using PYTHON scripts, and is submitted to ABAQUS for an analysis. The relevant responses are extracted by parsing individual analysis output files. This allows for an automated workflow, which is essential for optimization. VisualDoc supports various design optimization approaches, such as, global optimization (particle swarm or genetic algorithms) and gradient-based optimization.

Damage tolerance analysis requires that a crack be present in the structure. *The Joint Service Specification Guide* [11] specifies a minimum initial crack size of 0.127 mm to exist in the structure at all time. However, we considered a more conservative value of 0.2 mm for the initial crack size [12]. The crack is introduced at the most critical region (highly-stressed region), which is determined by static stress analysis [7].

The optimization problem is formulated as

$$\begin{aligned} &\min_{\mathbf{x}} f_0(\mathbf{x}) \\ &f_i(\mathbf{x}) \le 1, \qquad i = 1, \ldots, m \\ &A_j \le x_j \le B_j, \qquad j = 1, \ldots, n \end{aligned} \tag{1}$$

where f_0 is the objective function to be minimized with respect to design variables $\mathbf{x}$, while satisfying the constraints f_i. The design variables indicated by $\mathbf{x}$ are bound by side constraints in the form of upper limits (B_j) and lower limits (A_j). In the present study the structural mass is used as the objective function and constraints are imposed on damage tolerance stress intensity factor K, the buckling load factor, maximum von Mises stress, and the crippling stress in stiffeners. Design variables include stiffener shape (orientation and curvature) and sizing variables (heights and thicknesses of stiffener webs and flanges) for the stiffeners and panel thickness. Additional

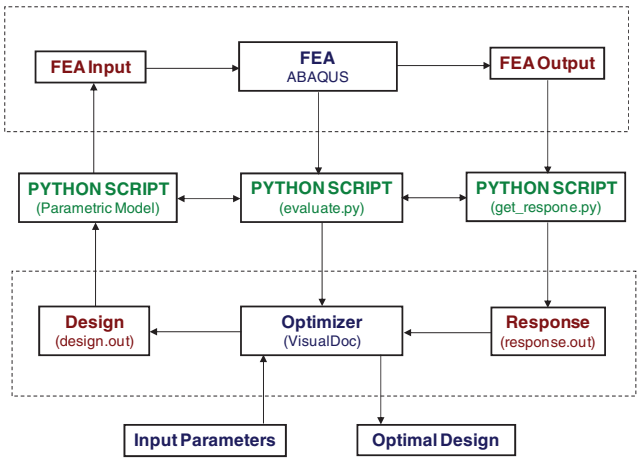

Fig. 2 Framework for optimization problem with multiconstraints.

thickness design variables are prescribed for each pocket created by stiffener intersection and panel boundary.

B. Response Evaluation

The linear buckling analysis is performed using the buckle procedure from ABAQUS that returns the lowest buckling eigenvalues or the critical buckling load factor. The von Mises stress distribution as well as crippling stress are calculated from the static analysis procedure, and the stress intensity factor is obtained from the contour integral calculation, both in ABAQUS. With this information, the constraints are formulated as follows.

1) Buckling constraint:

$$\text{Critical buckling load factor } \lambda_o \geq 1$$
$$\frac{1}{\lambda_o} \leq 1 \tag{2}$$

where λ_o is the lowest value of eigenvalues that we obtained from solving the eigenvalue problem;

2) von Mises stress constraint:

$$\sigma_{\text{VM}}(\text{von Mises stress}) \leq \sigma_Y(\text{yield stress})$$
$$\frac{\sigma_{\text{VM}}}{\sigma_Y} \leq 1 \tag{3}$$

Ideally, a stress constraint for each element would be specified. However, due to the inclusion of shape design variables, the finite-element (FE) mesh topology changes for every design point. In such cases, either the maximum constraint value or an aggregated constraint value over the entire FE mesh can be used. Since a maximum constraint value might display a discontinuous behavior, the present work uses the Kreisselmeir–Steinhauser criteria [13] for constraint aggregation:

$$\text{KS}(\mathbf{f}) = \frac{1}{\rho}\ell_n\left(\frac{1}{\sum_{i=1}^{N} A_i}\sum_{i=1}^{N} A_i e^{\rho f_i}\right) \leq \sigma_Y \tag{4}$$

where, f_i is the constraint in the ith element, ρ is a constant whose value changes the behavior of the constraint. For example, a high ρ value tends to direct the constraint value towards a maximum and a low ρ value tends to direct the constraint value towards the average. In the present implementation, a rather high value, 150, is used. Additionally, to avoid stress concentrations localized in very small areas, a weighted average is taken using individual element areas (A_i) in the FE mesh.

1) Damage tolerance constraint:

$$K_{\text{eff}} \leq K_{\text{IC}} \tag{5}$$

where K_{IC} is the plane strain fracture toughness [14]. The effective stress intensity factor K_{eff} is computed as

$$K_{\text{eff}} = \sqrt{K_I^2 + \alpha K_{II}^2} \quad \text{where } 0 \leq \alpha \leq 1 \tag{6}$$

where K_I and K_{II} are Mode 1 and Mode 2 stress intensity factor, respectively. α is an empirical coefficient that scales the contribution from the additional stress intensity factors, and is assumed to be one for this study.

2) Crippling constraint: for structures with stiffeners, one often checks the crippling strength of stiffeners. This, is calculated as

$$\sigma_{\text{rep}}^{s} \leq \sigma_C \tag{7}$$

where $\sigma_{\text{axial}}^{s}$ is a representative stress measure for the stiffener and we estimated this representative stress measure to be the von Mises stress in the stiffener, σ_C is the crippling strength [15] and is computed for a stiffener with one edge free as

$$\sigma_C = \frac{0.61525.\sigma_Y}{(X)^{0.783387}} \quad \text{and} \quad \sigma_C \leq \sigma_Y \quad \text{where } X = \frac{b}{t}\sqrt{\frac{\sigma_Y}{E}} \tag{8}$$

where, σ_Y is the yield strength of the material, b and t are the height and thickness of the stiffener, respectively, and E is the Young's modulus. If the stress σ_C exceeds σ_Y then σ_Y should be used.

C. Parametric Model

The optimization problem considered in this paper is that of a stiffened panel with curved stiffeners. Two different cases are considered: first, a panel with two stiffeners and one cutout, and second a panel with four stiffeners and two cutouts. In both cases the panel has a rectangular planform. The baseline panel configuration, loading, material properties, and design constraints are provided by Lockheed Martin Aeronautics Company, and are representative of typical aircraft structures. The material properties used for the two-stiffener design were for Al 7050-T7451, and for the four-stiffener design were for Al 2139. The stiffeners are assumed to have a blade cross-section, and each circular cutout is ring-stiffened by providing a region of higher thickness around it. The sizing design variables include height and thickness of individual stiffeners, subpanel thickness in each pocket created by intersecting stiffeners, and the thickness and width of each ring around the panel cutout. In addition to this, shape design variables are used to parameterize the shape and curvature of the stiffener.

Controlling the shape of the stiffener curve posed a few challenges due to the geometry modeling limitations of ABAQUS CAE module. CAE creates a spline interpolation curve using predefined control points. Because of the nature of spline interpolation it is difficult to ensure that its convex-hull, which here is created using three control points, lies within the panel boundaries. This creates a possibility that for some combinations of the shape design variables, the curve may lie outside the panel. This would create an invalid configuration. This problem is solved by a combination of a two-step interpolation scheme and carefully chosen bounds on shape design variables. First, the shape design variables are used to create a control polygon, through which a Bezier curve is created. The control points for the spline interpolation inside CAE are then obtained from this curve. Since it is easy to ensure that the control polygon lies within the panel boundaries, the chances of the resulting curve created inside CAE are greatly reduced. The Bezier curve (see Fig. 3a) in the parametric form is written as

$$\begin{Bmatrix} x \\ y \end{Bmatrix} = (1-t)^2\begin{Bmatrix} x_i \\ y_i \end{Bmatrix} + 2t(1-t)\begin{Bmatrix} x_j \\ y_j \end{Bmatrix} + t^2\begin{Bmatrix} x_k \\ y_k \end{Bmatrix} \tag{9}$$

where $t \in [0, 1]$, and (x_i, y_i), (x_j, y_j), (x_k, y_k) are coordinates of the control points i, j, and k, respectively.

To create a curve in ABAQUS using Spline interpolation technique, we use three points from the Bezier curve at $t = 0$, 0.5, and 1, shown as (x_i, y_i), (x_m, y_m), (x_k, y_k), respectively. The spline interpolation is then created using these three points (see Fig. 3b). Because of differences in formulations of the two curves, the spline curve created in CAE may still go outside the domain of the plate boundaries, but the formulation ensures that this happens for extreme combinations of the design variables. Hence, appropriate bounds chosen on the location of the control points i, j, and k could ensure that the curve stays within the panel boundary. This approach requires 4 shape design variables per stiffener: x- and y- coordinates of point J, and the boundary location of points I and K.

A script to build a parametric model of stiffened plate is created using Marco Manager in ABAQUS, which records a sequence of operations in a PYTHON script. This is done for one configuration of the stiffened panel and following this, all numbers in the script that relate to the design variables are labeled using variable names. This script is called *stiffened_plate.py.template* (see Fig. 1), and is responsible for creation of analysis model, execution of analysis and extraction of results from output file. For analysis at each design point, these variables are replaced with their numerical values from the optimizer.

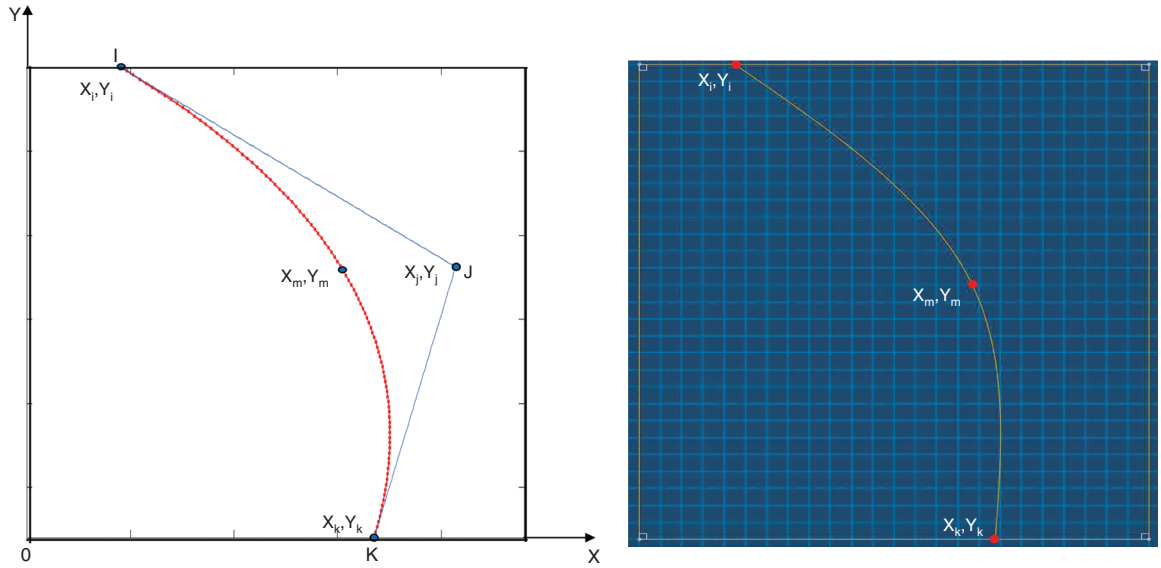

a) Create a bezier curve using three control points b) Create a spline through three points in ABAQUS

Fig. 3 Method to create a curvilinear stiffener in ABAQUS.

III. Design Examples

A. Optimization of Cracked Panels with an Elliptic Hole

In this design example, we perform the optimization of a stiffened panel with damage tolerance and buckling constraints only. The given example is an illustrative one to show that buckling phenomenon can happen for panels with defects under tension, and buckling modes are expected to be mostly local around defects (cracks or holes). Only straight stiffeners are considered and the panel loading and boundary conditions are shown in Fig. 4. It can be seen that the tension loading along the x_2 direction is dominant. The panel has an elliptic hole located at the center of the panel.

It can be easily verified that the region of high stress on the panel are the edge of the major axis of the elliptic hole, which is perpendicular to the tension loading N_2. A crack of minimum size is placed at this location. As explained earlier, the minimum crack length is taken to be 0.2 mm. The weight of the panel is minimized under constraints on static fracture strength and buckling eigenvalue, and design variables x_1 to x_8 as shown in Fig. 4.

The cracked stiffened panel is modeled in ABAQUS using shell finite elements. To get the accurate stress intensity factor, a very fine mesh is used at the crack tips. To create this fine mesh, a rectangular box with a mesh size of 0.008 mm is created around the crack. The stress intensity factors are calculated around 25 contours defined inside this box. This gives an indication about the convergence of the integral, and the 24th contour integration is used. To reduce the computational costs, a gradually varying mesh size is used from the fine mesh around the crack tip to the rest of the computational domain. A coarser computational mesh is used for the buckling analysis. Figure 5 shows the optimization history for the objective function (weight) and the damage tolerance constraint on static fracture strength using the particle swarm optimization (PSO) algorithm with 40 particles. The CPU time for this optimization task is reported as FEAs = 5759; 38 h 50 min for 99 iterations CPU Q 6850, 2.99 GHz, 3.25 GB Ram. The PSO design history shows that the mass and damage tolerance constraint converged after 20 iterations. The PSO optimization result is then used as a starting point for the gradient-based optimization (see Fig. 6), which reaches

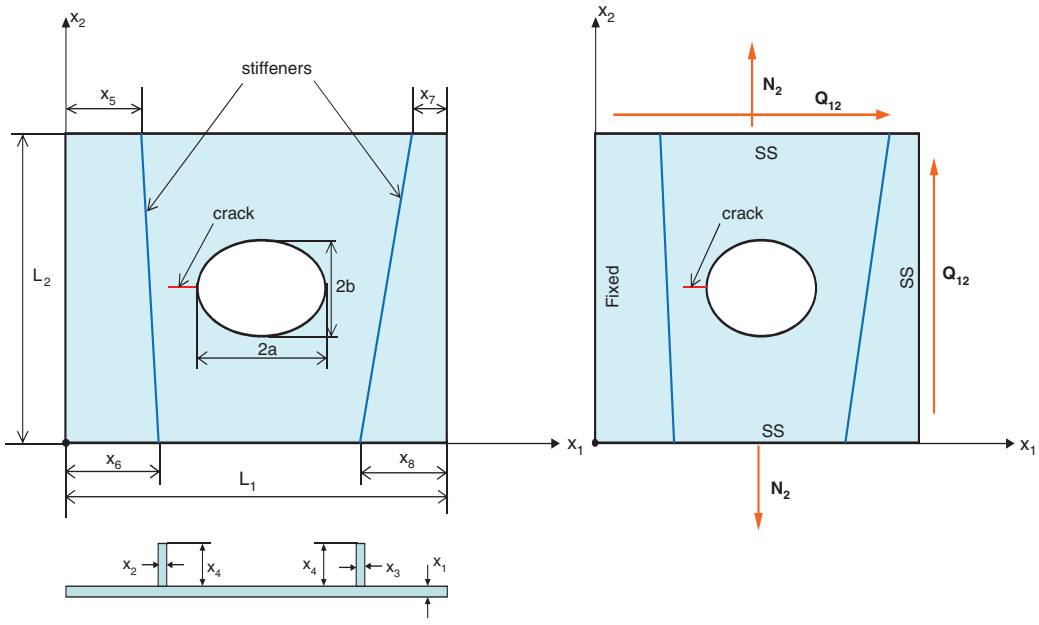

Fig. 4 Design variables, loading schematic and boundary conditions: $L_1 = 0.5080$ m, $L_2 = 0.4064$ m, $a = 0.06$ m, $b = 0.04$ m. $N_2 = 770,000$ N/m, $Q_{12} = 9000$ N/m. Material Al 7050-T7451.

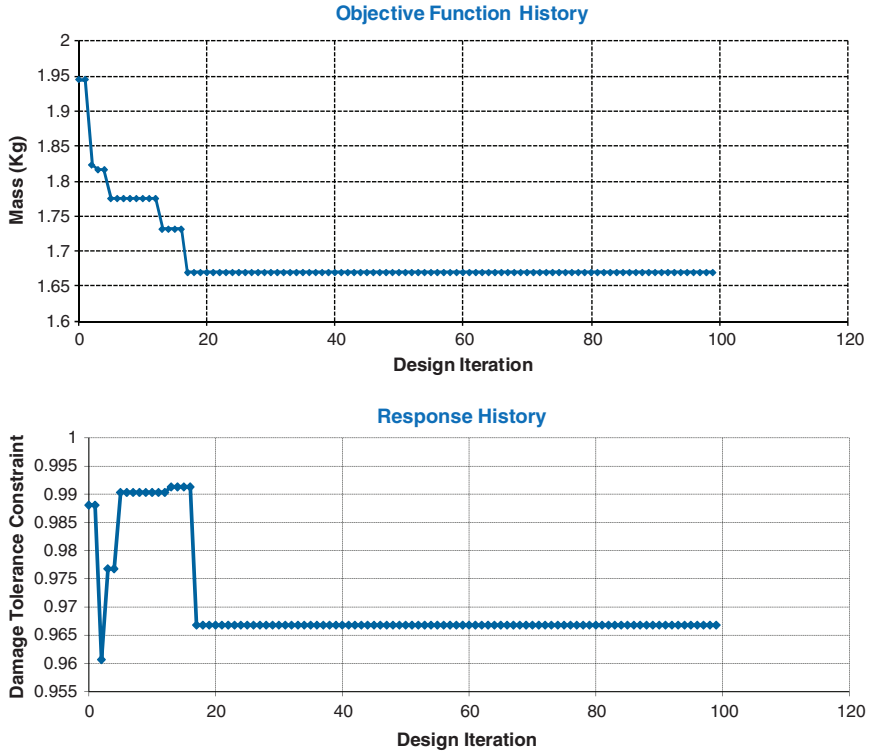

Fig. 5 Optimization history for the objective function (mass) and constraint for optimization of the cracked stiffened panel using the PSO algorithm.

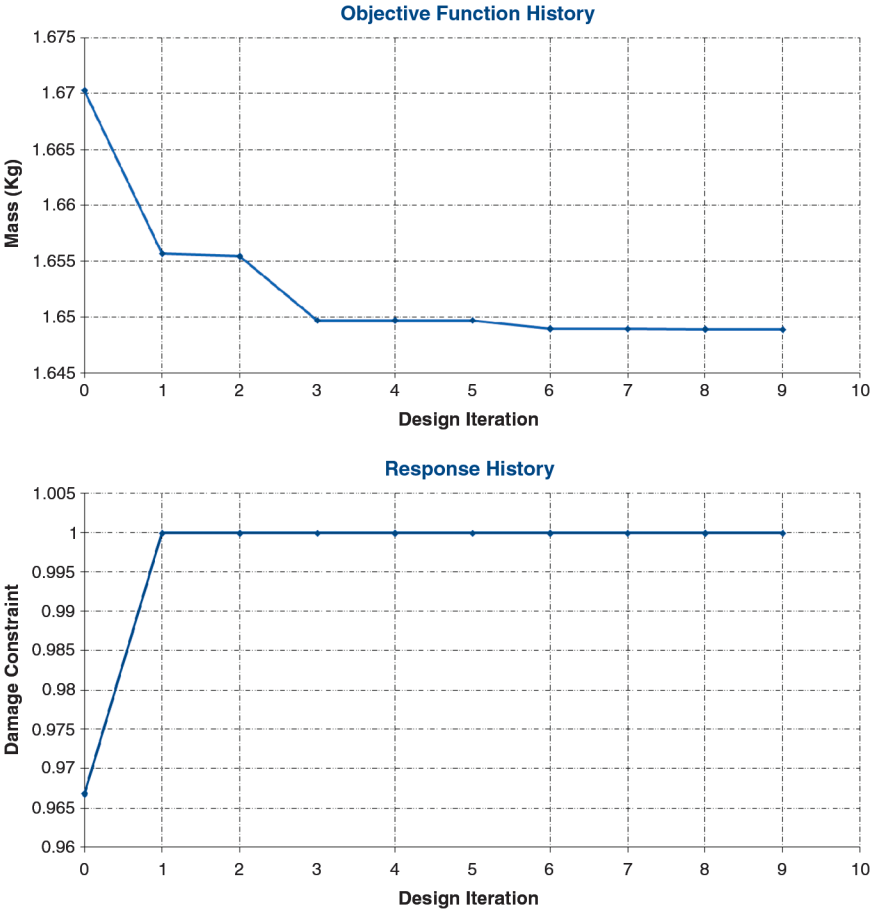

Fig. 6 Optimization history for the objective function (mass) and damage constraint for optimization of cracked stiffened panel using the gradient-based optimization (GBO) algorithm with nine iterations.

Table 1 Optimization results for the cracked stiffened panel with an elliptic hole under damage tolerance constraint using the PSO algorithm

	Optimal design	Starting point design
Optimum weight	1.649 kg	1.925 kg
Optimum skin thickness	2.764 mm	3.175 mm
Constraint on damage	0.99997	——
Constraint on buckling	0.82857	——

convergence in nine iterations with FEAs = 153 and CPU time = 54 minutes on the same computer. The optimization results are listed in Table 1, and the optimal design configuration is shown in Fig. 7. The optimal design variable values are $x_1 = 2.764$ mm, $x_2 = 8.00$ mm, $x_3 = 1.00$ mm, $x_4 = 16.543$ mm, $x_5 = 172.00$ mm, $x_6 = 172.00$ mm, $x7 = 24.536$ mm, $x_8 = 135.598$ mm. The optimal position of one of the stiffeners (x_5 and x_6) and its thickness (x_2) are at the upper bounds of x_5, x_6 and x_2. This stiffener is very close to the crack (see Fig. 6), and the direction of the stiffener is perpendicular to the crack, thus playing the role of a damage arresting mechanism. While x_3, the thickness of the stiffener (x_7 and x_8), obtained is at its lower bound, this stiffener does not have any influence on arresting the crack.

Figure 8 shows the first four buckling modes of the optimal design, and it shows that the panel could loose stability even under tensile loading. We can realize that the buckling modes are mostly local around the hole in nature. Therefore, in practical design, reinforcements around locally weak areas, such as cracks and holes could be used to withstand failure modes due to both bucking and damage. For example, ring-stiffening around cutouts is a commonly used form of reinforcement, and is studied in the next design case. This example was suggested by Lockheed Martin Aeronautics as a potential case for which curvilinear stiffeners may be appropriate.

B. Optimization of Curvilinear-Stiffened Panel with Multiconstraints under Multiload Cases

1. *Lockheed Martin Baseline Presentation*

The baseline panel shown in Fig. 9 is considered in this study. The panel has fixed-fixed boundary conditions with two cutouts under two load cases (see Fig. 10). The first load case (Fig. 10a) is compression dominant and the second (Fig. 10b) is tension dominant load case. The following constraints for each load cases are considered: buckling, damage tolerance, von Mises stress, crippling and the consideration of durability cutout stress which is called DaDT considerations. The response on the consideration of durability cutout stress will be the maximum principal stress at cutouts and is imposed to be less than $0.5\sigma_Y$, the constraint on crippling is checked for the optimal design. The panel is designed with one ring around each cutout and two separate optimization studies are performed two and four curvilinear stiffeners, respectively. The results from each optimization are discussed below.

2. *Optimization Results of Lockheed Martin Baseline with Two Curvilinear Stiffeners*

Optimization results of panel shown in see Fig. 9 with two stiffeners is presented here. In this design example, stiffeners are designed, so that they do to not intersect each other and are not allowed to cross over the cutouts, therefore the appropriate range of design variables needs to be determined, the design variable scheme is shown in Fig. 11 and the results are summarized in Table 2.

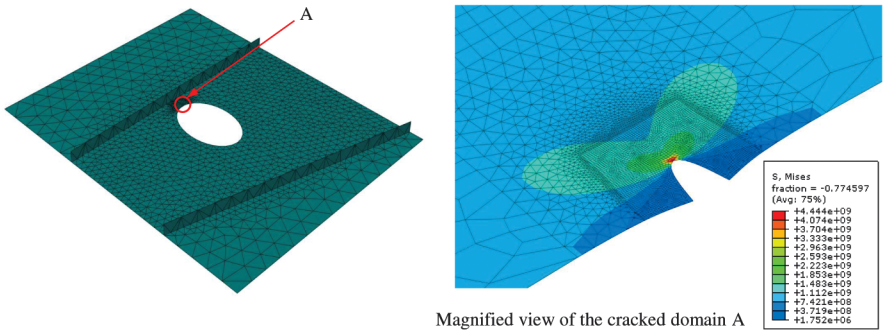

Fig. 7 Optimal design configuration for optimization of the stiffened panel with an elliptic hole.

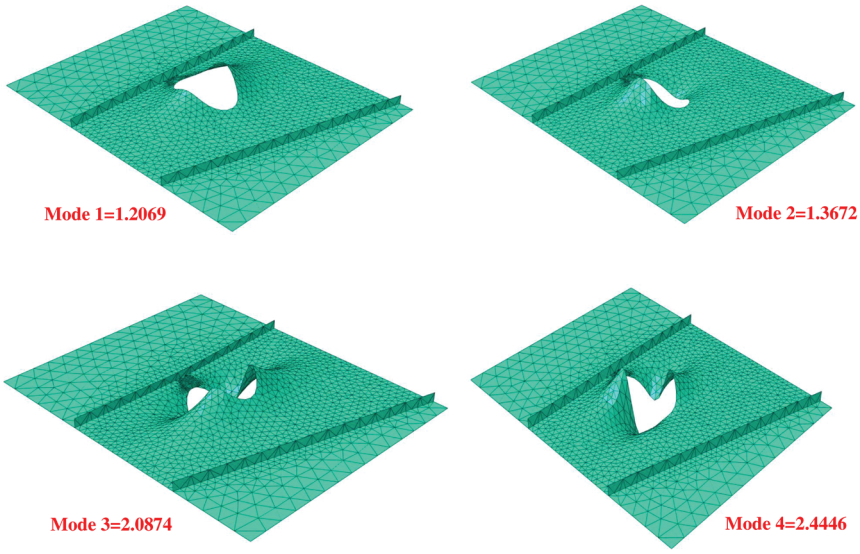

Fig. 8 First four buckling mode shape of cracked stiffened panel.

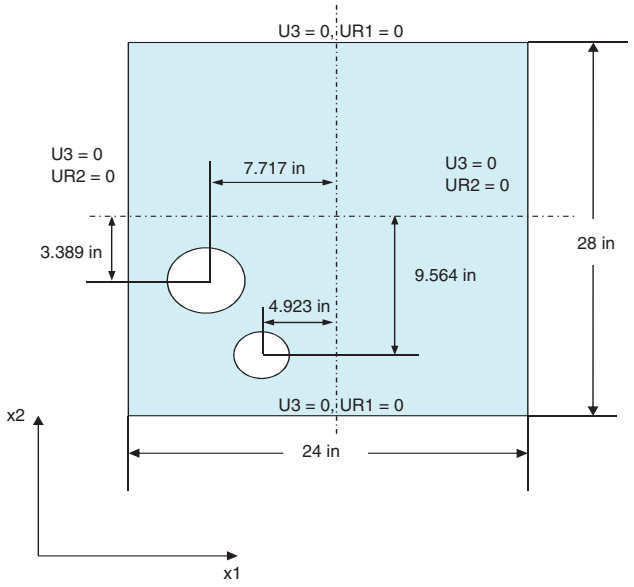

Fig. 9 Lockheed Martin baseline with fixed boundary conditions.

The buckling constraint is active, while the ones on von Mises stress and damage tolerance are not. In this study, the damage tolerance constraint value of 0.0806 shows that it was satisfied by a large margin. Additionally, the crippling constraint and DaDT criterion are also satisfied with values of 0.807 and 0.7436, respectively. This result was used to serve as a basis to decide that the damage tolerance constraint not be included in the optimization of panel with four stiffeners. This constraint is expected to have a low value for the four-stiffener case, and hence ignoring it during the course of optimization would not influence the nature of results. However, a significant reduction of CPU time is obtained.

Table 3 shows the optimal parameters for all 17 design variables, and the optimal configuration is shown in Fig. 12. Lockheed Martin's experience suggests that the ring thickness should be less than 3 times the panel skin thickness (2.5867 mm). This is also seen in the current optimal design. The first four buckling mode shapes of this configuration are shown in Fig. 13. It is seen that the eigenvalues of the first four buckling mode are very closely clustered. The optimization is carried out using the PSO with 40 particles and convergence was reached in 69 iterations (see Fig. 14). The PSO optimization result is then used as a starting point for the gradient-based optimization (see Fig. 15), which reaches convergence in 8 iterations.

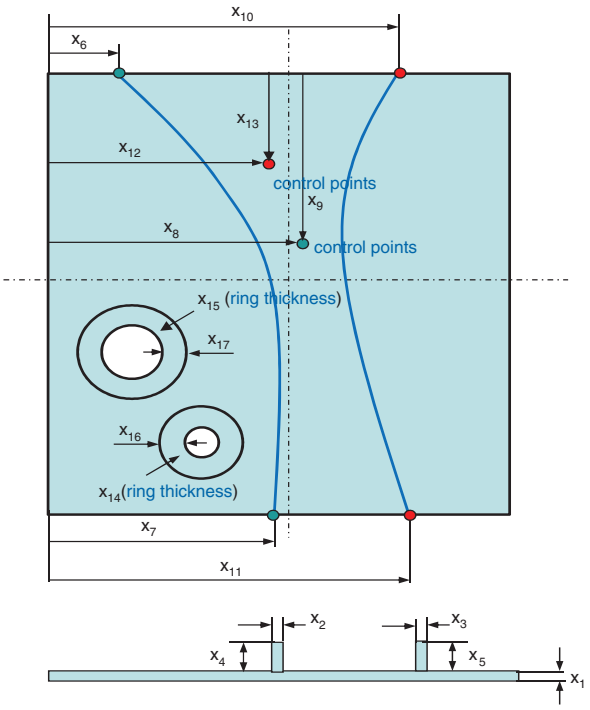

Fig. 11 Design variables for optimization problem with two curvilinear stiffeners.

3. Optimization Results of Lockheed Martin Baseline with Four Curvilinear Stiffeners

This section presents the design of panel shown in Fig. 9 with four curvilinear stiffeners. The constraints on buckling, von Mises stress, and DaDT are included in optimization, while the damage tolerance constraint and crippling are checked post-optimization. This results in a significant reduction in CPU time. In the current framework, stiffeners are designed not to cross over the cutouts, a total of 34 variables are used, to parameterize the design, and are shown in Fig. 16. However, out of these, only 32 are used in optimization, and X_{33} and X_{34} are held fixed. This is because the stiffener parameterized by variables X_{31}-X_{34} is required to pass through the narrow region between the two rings. Hence, the location of X_{33}, X_{34} are fixed and only X_{31} and X_{32} are allowed to vary for this stiffener. Because of this constraint, this stiffener curve is created using a pure spline function in ABAQUS CAE, while the remaining three stiffener curves are created using the two-step approach described earlier. In this design, the stiffeners are designed to generate nine domains which are in

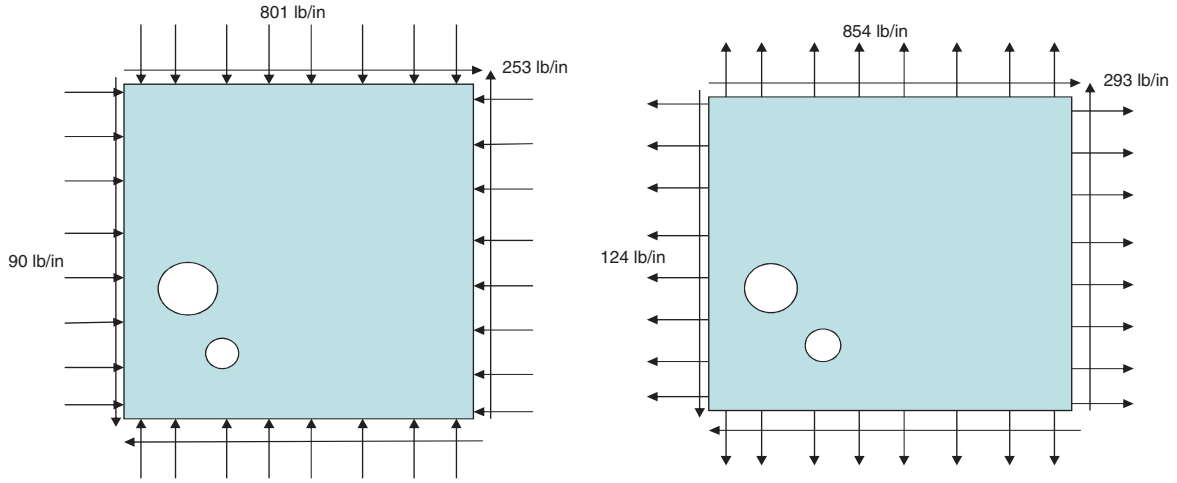

a) Maximum compression load case **b) Maximum tension load case**

Fig. 10 Baseline under multiload cases.

Table 2 Optimization results for Lockheed Martin cutout-panel with multiconstraints under multiload: two-curvilinear-stiffener case

	Mass	Crippling constraint	DaDT constraint	Stress constraint	Buckling constraint	Damage tolerance constraint
Optimal design	7.28 lb (3.30 kg)	0.807	0.744	0.361	1.000	0.081

Table 3 Optimal design variables for Lockheed Martin cutout panel with multiconstraints under multiload cases: two-curvilinear-stiffener case

Design variable	Meaning	Low bound, in.	Upper bound, in.	Optimal design, in.
X1	Skin thickness	0.063	0.177	0.1018
X2	Stiffener thickness 1	0.063	0.315	0.0639
X3	Stiffener thickness 2	0.063	0.315	0.0630
X4	Stiffener height 1	0.394	1.97	1.1473
X5	Stiffener height 2	0.394	1.97	1.5059
X6	Control point end	0.27	11.5	5.4368
X7	Control point end	9.7	11.5	10.7631
X8	Control point mid	9.7	11.5	9.7533
X9	Control point mid	0.27	14	13.3645
X10	Control point end	12	23.2	12.5000
X11	Control point end	12	23.2	16.7639
X12	Control point mid	12	23.2	19.7008
X13	Control point mid	0.27	27.73	24.8921
X14	Ring thickness for small hole	0.063	0.315	0.2957
X15	Ring thickness for big hole	0.063	0.315	0.1672
X16	Ring width for small hole	0.4	1.6	0.8176
X17	Ring width for big hole	0.4	1.6	1.3669

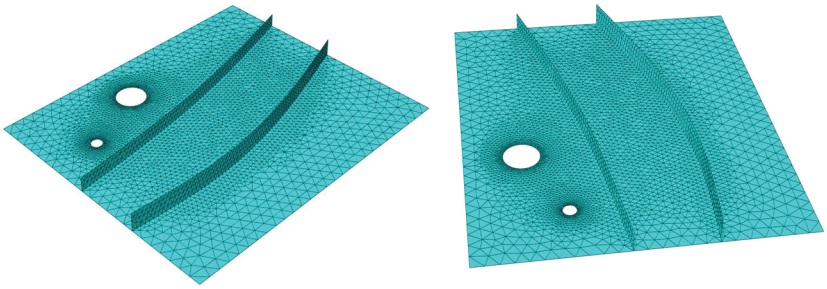

Fig. 12 Optimal design configuration for Lockheed Martin panel using PSO and gradient-based optimization: two-curvilinear-stiffener case.

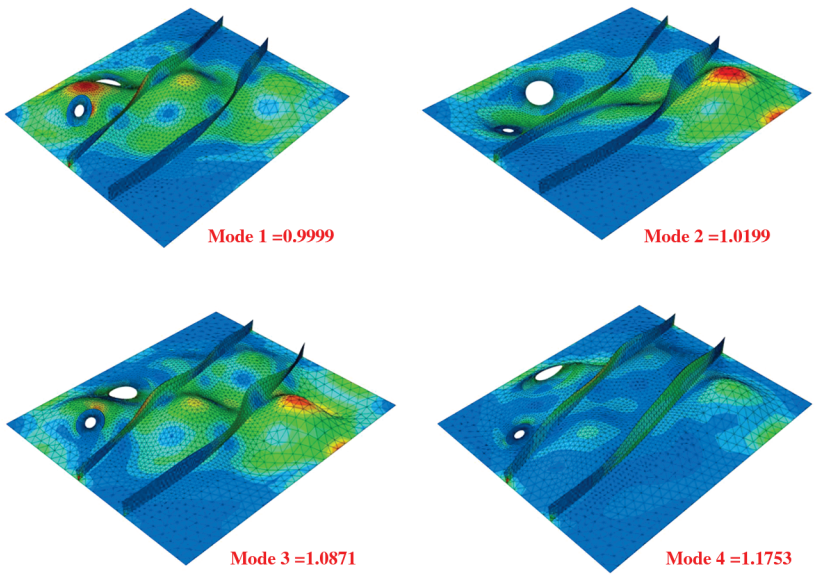

Fig. 13 First four buckling mode shapes of optimal design configuration using two curvilinear stiffeners.

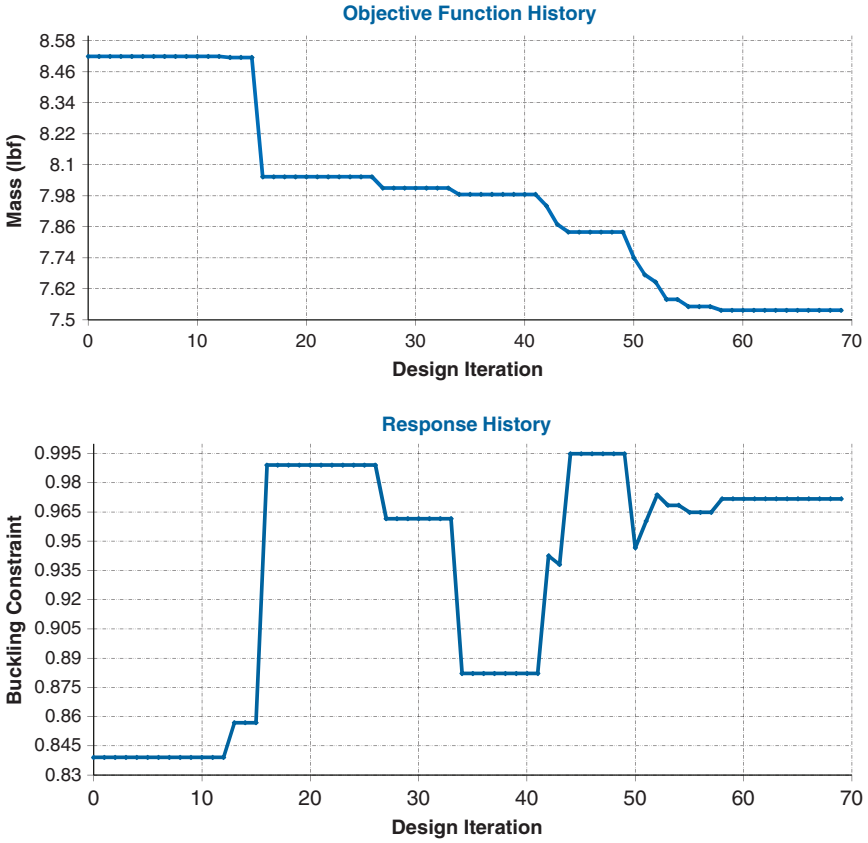

Fig. 14 Optimization history for the objective function (mass) and buckling constraint for optimization of Lockheed Martin panel using the PSO algorithm with 69 iterations.

between stiffeners and panel boundaries, thus a nonuniform thickness distribution is allowed by using different panel thicknesses in these domains (X_1-X_9). This is helpful since in most cases the critical buckling modes are local in nature, and a nonuniform thickness distribution could help in local stiffening to achieve a lower panel mass.

The results were obtained using genetic algorithm. Tables 4 and 5 list the converged optimization results for the panel under

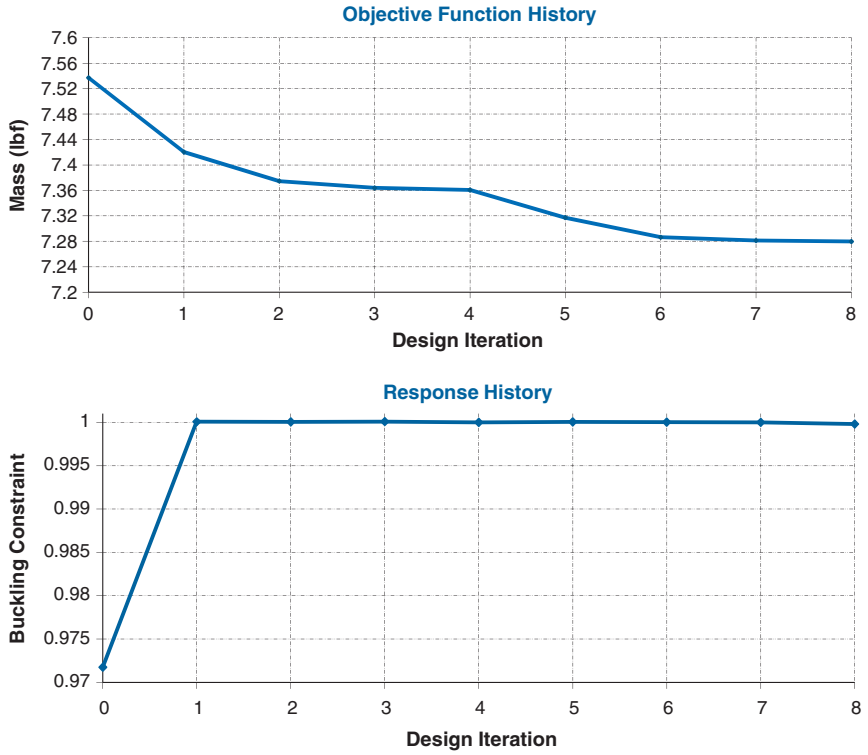

Fig. 15 Optimization history for the objective function (mass) and buckling constraint for optimization of Lockheed Martin panel using the GBO algorithm with eight iterations.

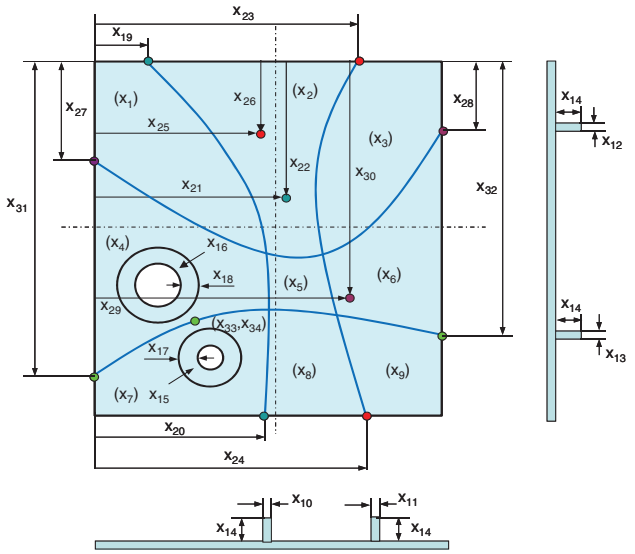

Fig. 16 Design variables for optimization problem with four curvilinear stiffeners.

consideration. The optimal design with four curvilinear stiffeners has approximately 6% lower mass than that using two curvilinear stiffeners discussed in the previous section. For the current design, the DaDT and buckling constraints become active, and the constraint on damage tolerance is 0.7326. Except for the ring thickness around the bigger hole, the size and thickness of rings around cutouts are less than for the design with two curvilinear stiffeners. Figure 17 shows the thickness of subpanel regions, stiffeners and rings around cutouts.

Figure 18 gives the contour of von Mises stress and the location of maximum von Mises stress appears at the edge of the subpanel which has the lowest thickness. The first nine buckling mode shapes and their eigenvalues are presented in Fig. 19. It is seen that the first buckling mode is a combined global and local mode, while the remaining buckling modes are local in nature. Additionally, the eigenvalues are seen to be very closely clustered, which leads to the possibility of mode switching with small variations of design variables.

4. Comparison of the Current Optimal Design with Lockheed Martin's Industry-Standard Design

To demonstrate the effectiveness and advanced features of the current framework of stiffened unitized structures the optimization results are compared with the Lockheed Martin's industry-standard design, shown in Fig. 20. The current optimal design is approximately 7% lighter than Lockheed Martin industry-standard design,

Table 4 Optimization results for Lockheed Martin cutout panel with multiconstraints under multiload cases using genetic algorithm: four-curvilinear-stiffener case

	Mass	DaDT constraint	Crippling constraint	Stress constraint	Buckling constraint	Damage tolerance constraint
Optimal design	6.850 lb (3.10 kg)	0.942	0.098	0.465	1.004	0.734

Table 5 Optimal design variables for Lockheed Martin cutout-panel with multiconstraints under multiload cases using genetic algorithm: four-curvilinear-stiffener case

Design variable	Meaning	Low bound, in.	Upper bound, in.	Optimal design, in.
X1	Skin thickness	0.0394	0.158	0.0978
X2	Skin thickness	0.0394	0.158	0.0434
X3	Skin thickness	0.0394	0.158	0.0890
X4	Skin thickness	0.0394	0.158	0.1160
X5	Skin thickness	0.0394	0.158	0.0741
X6	Skin thickness	0.0394	0.158	0.0886
X7	Skin thickness	0.0394	0.158	0.0862
X8	Skin thickness	0.0394	0.158	0.0735
X9	Skin thickness	0.0394	0.158	0.0692
X10	Stiffener thickness 1	0.0394	0.315	0.2774
X11	Stiffener thickness 2	0.0394	0.315	0.1839
X12	Stiffener thickness 3	0.0394	0.315	0.0964
X13	Stiffener thickness 4	0.0394	0.315	0.0785
X14	Height of stiffeners	0.394	1.97	0.5295
X15	Ring thickness for small hole	0.0394	0.315	0.1868
X16	Ring thickness for big hole	0.0394	0.315	0.2342
X17	Ring width for small hole	0.4	1.6	0.4166
X18	Ring width for big hole	0.4	1.6	0.4009
X19	Control point end stiffener 1	0.8	11.5	11.4994
X20	Control point end stiffener 1	9.7	11.5	10.6650
X21	Middle control point stiffener 1	9.7	11.5	10.7693
X22	Middle control point stiffener 1	0.8	14	4.9593
X23	Control point end stiffener 2	12.5	23.2	14.1542
X24	Control point end stiffener 2	12.5	23.2	16.3251
X25	Middle control point stiffener 2	12.5	23.2	18.7687
X26	Middle control point stiffener 2	0.8	27.2	21.5035
X27	Control point end stiffener 3	0.8	14.2	6.0528
X28	Control point end stiffener 3	0.8	13.6	10.3057
X29	Middle control point stiffener 3	0.8	23.2	3.9273
X30	Middle control point stiffener 3	0.8	14.2	3.5109
X31	Control point end stiffener 4	19.6	27.2	25.8652
X32	Control point end stiffener 4	14	27	24.5474

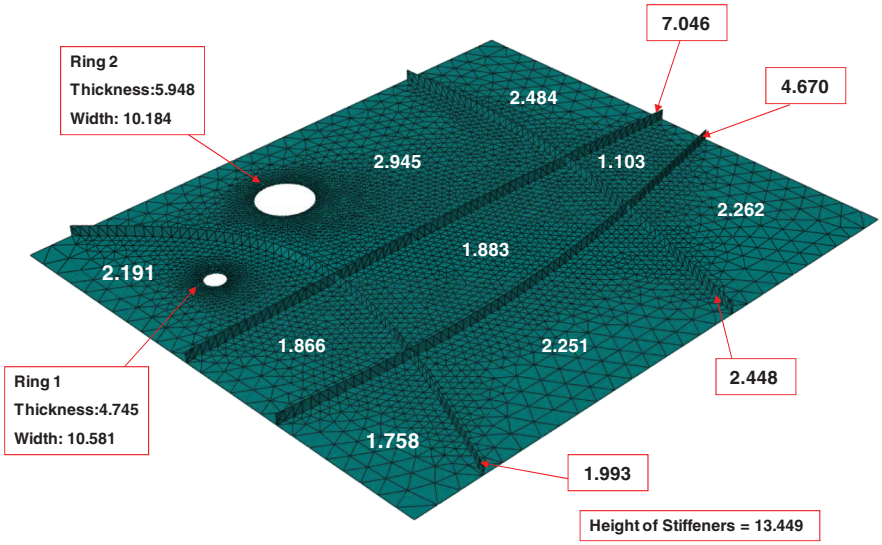

Fig. 17 Optimal design configuration and thickness of elements for Lockheed Martin panel using genetic algorithm: for the case of four curvilinear stiffeners.

and has the following innovations compared with Lockheed Martin's:

1) The design has four stiffeners to produce a lighter-weight solution than a two-stiffener design (approximately 6%).

2) The design includes cutouts as required for system penetrations on aircraft structure.

3) The design includes the addition of pad-ups around the cutouts as required for DaDT considerations.

4) The design optimization process includes damage tolerance analysis.

5) The design optimization included a stress constraint in the vicinity of the cutout which can be tailored to a durability cutoff stress (DaDT consideration).

6) The optimization process was performed over multiple load cases simultaneously. This is meant to design a structure that is optimized for several critical load cases (rather than a single load case and then manually redesigned for the other sizing cases).

7) The design optimization includes multiple design variables for nonuniform panel thicknesses. This is a significant feature for weight reduction as individual web bays can be tailored over the entire panel.

8) Optimization results with multiple constraints (buckling, DaDT, damage tolerance, crippling, stress, etc.) can be obtained using the current framework.

9) Curvilinear stiffeners are used, thus it is more flexible for curvilinear stiffeners to stiffen the appropriate domains. A four-stiffener design which will produce a lighter weight solution than a two-stiffener design (approximately 6%).

The mass of the optimal design with two curvilinear stiffeners (see Table 2), 3.30 (kg) using the design variable of uniform panel thickness, compared with that of Lockheed Martin, 3.337 (kg) using four straight stiffeners and the nonuniform panel thickness variables is a clear demonstration for this conclusion.

In the current paper, a genetic algorithm is used for the last design example of the optimization problem with 32 design variables. This is because the PSO had difficulties as performing the optimization problem with so many local optimum. Although the PSO is also a global optimizer, but choosing parameters in the PSO optimizer for a specific problem is critical (initial number of particles, velocity and relative position of each particle, etc.), the authors had some experience with PSO, for example using 40 particles as shown in the previous example has led to satisfactory results in terms of the converged results and computation time, but using the same parameters and a number of trial times failed for this problems. The genetic algorithm is in general a random search process with random outcome using discrete variables and has a capability to lead to the global optimum. It is very robust and easy to implement, but very inefficient. Optimization using the genetic algorithm can provide a number of good designs instead of a single optimum.

In general, for optimization problems with many local optima and with a large number of design variables, it is recommended that there should be an appropriate strategy before performing the optimization. For example, performing a parametric study to determine the possible relation of design variables, and using "smart" variables to reduce the number of design variables, and investigate relations

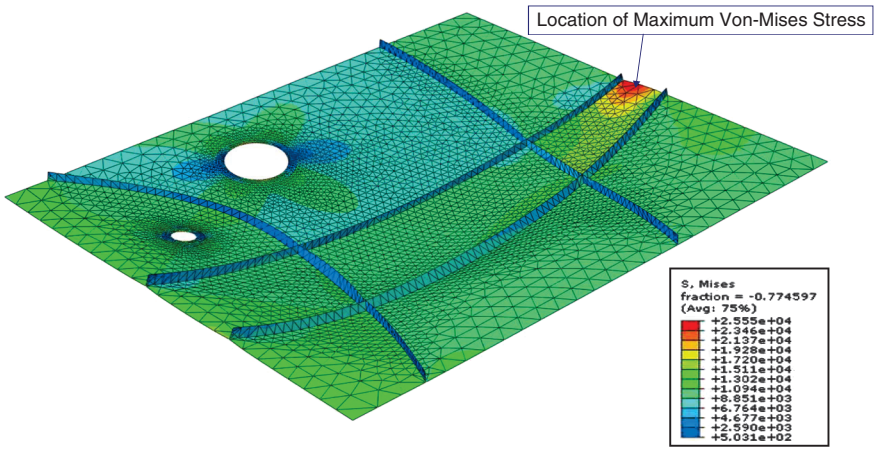

Fig. 18 Contour of von Mises stress of optimal design configuration: four-curvilinear-stiffener case.

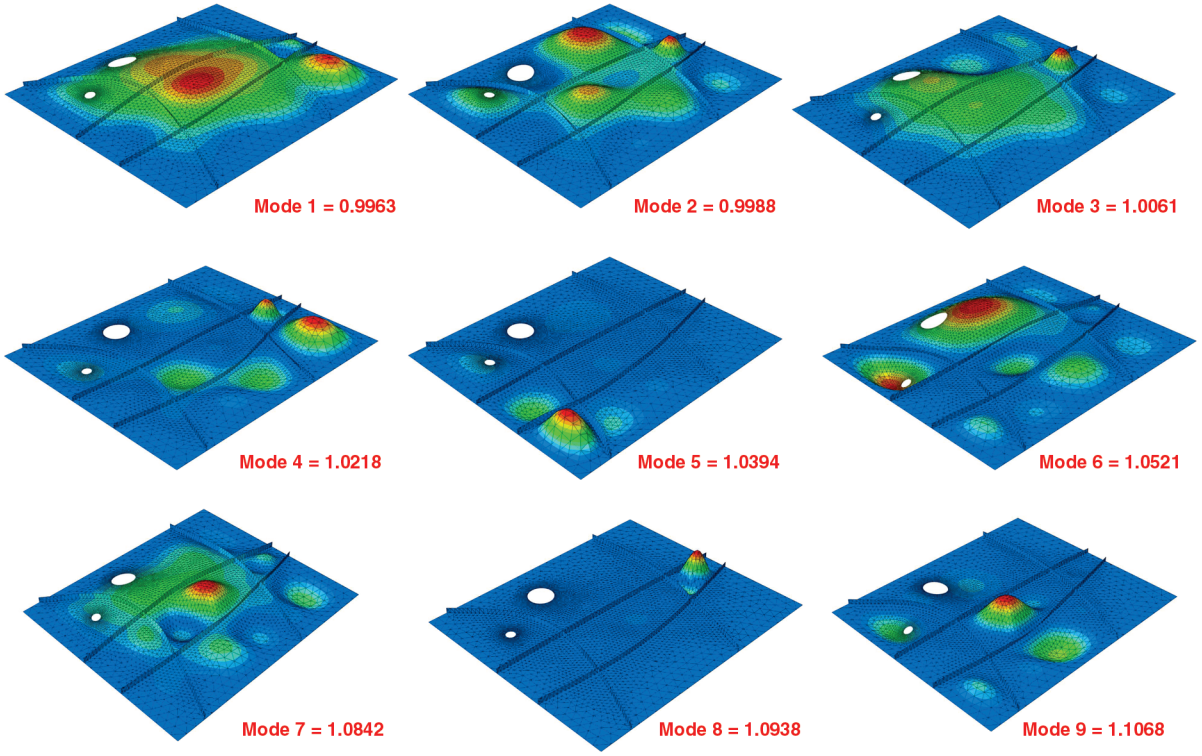

Fig. 19 First nine buckling mode shapes of optimal design configuration using genetic algorithm using four curvilinear stiffeners.

between various design variables and responses. A suitable combination of optimization algorithms with optimal parameters for this kind of the optimization problems is especially needed. There are also other difficulties encountered in the optimization process in the present study such as: A well known drawback of conventional finite element analysis in fracture mechanics is that to get accurate value of the stress intensity factor, a very fine mesh must be used at the crack tip region. This leads to an increase in the computational time for the optimization process. Also, when the shape variables are included in the optimization problem, the finite element mesh topology will vary for each analysis, this could lead to a change of mesh size at the crack tip region while the response on damage tolerance is very sensitive to mesh size at the crack tip region and thus the responses obtained may not be accurate. Thus mesh size should be fixed at this region in ABAQUS. In addition, for complex stiffened panels with cutouts and cracks along with stiffeners, geometry modeling becomes critical, and thus, determine the range of design variables is important. The stiffeners should not go over any part of the boundary of the panel and should not intersect the crack tip region. While letting the stiffeners be as free as possible to cover the whole design space. If the stiffeners intersect the crack tip region, mesh size in this region will vary after each analysis and the response on damage tolerance may not be accurate. It is noted that the crack tip region is a very small region, thus this constraint does not affect much on the outcome of the optimization problem.

IV. Postbuckling Response of Four-Stiffener Design in Combined Compression-Shear Test Fixture

To validate the four-stiffener panel design, a full scale panel has been fabricated and will be tested at NASA Langley Research Center in the combined compression-shear test fixture [10]. The test fixture has been designed to facilitate application of combined compression-

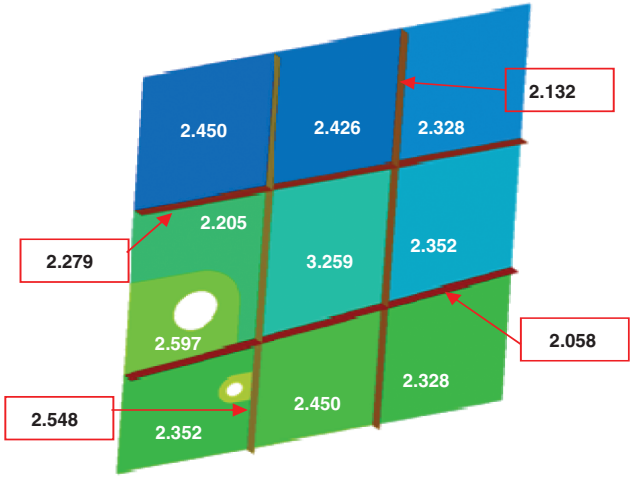

Fig. 20 Lockheed Martin's industry-standard panel with mass = 3.337 kg (7.35 lb) using the same baseline.

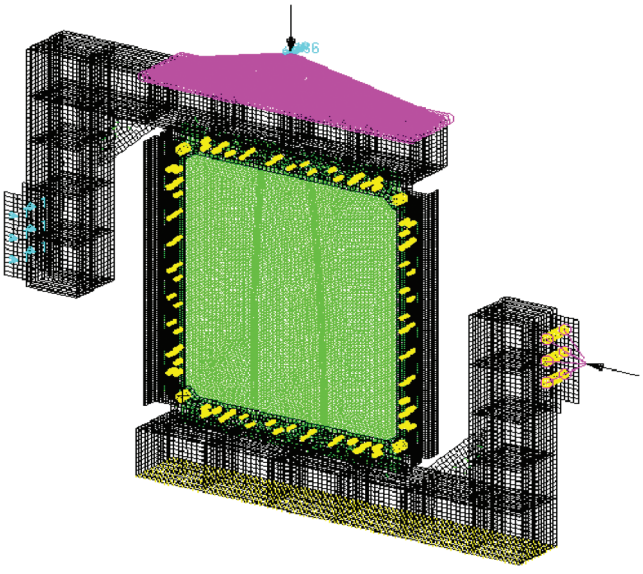

Fig. 21 Nonlinear test fixture model developed of the combined compression-shear test fixture at NASA Langley Research Center [16].

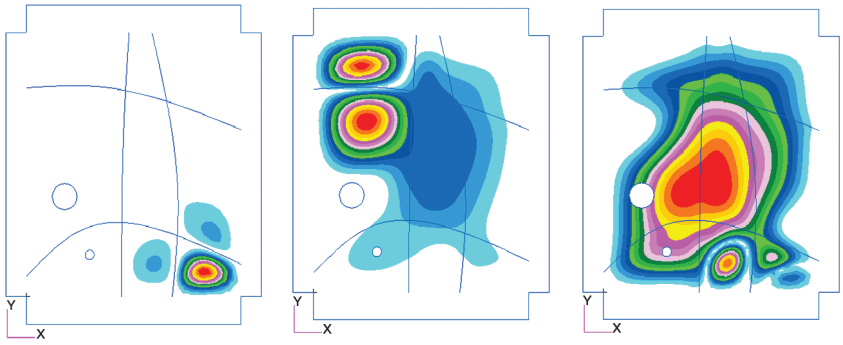

Fig. 22 First three mode shapes of four-stiffener panel using test fixture superelement to apply boundary conditions and loads.

shear loading; however, previous testing has shown that the boundary conditions and loading are not the ideal clamped conditions and uniform compression-shear loading to which the panel was designed [16]. The panel will be loaded beyond buckling until failure for the compression-dominate load case.

Analysis of the panel and test fixture were performed to obtain preliminary predictions for the expected panel response. A nonlinear finite element model (MSC Nastran) of the test fixture model was developed by Lockheed Martin and may be seen in Fig. 21. For details regarding the development of the nonlinear finite element test fixture model refer to Bird et al. [16]. The ABAQUS model was translated to MSC Nastran and interfaces were created to facilitate interaction between the test fixture model and the panel model. By using high fidelity modeling of the test fixture and interfaces, the nonlinear finite element model provided baseline predictions for the experimental predictions.

The linear buckling modes of the panel in the test fixture were extracted using a linear panel model and a reduced grid-point interaction superelement of the nonlinear test fixture model. The loading applied through the test fixture was statically equivalent to

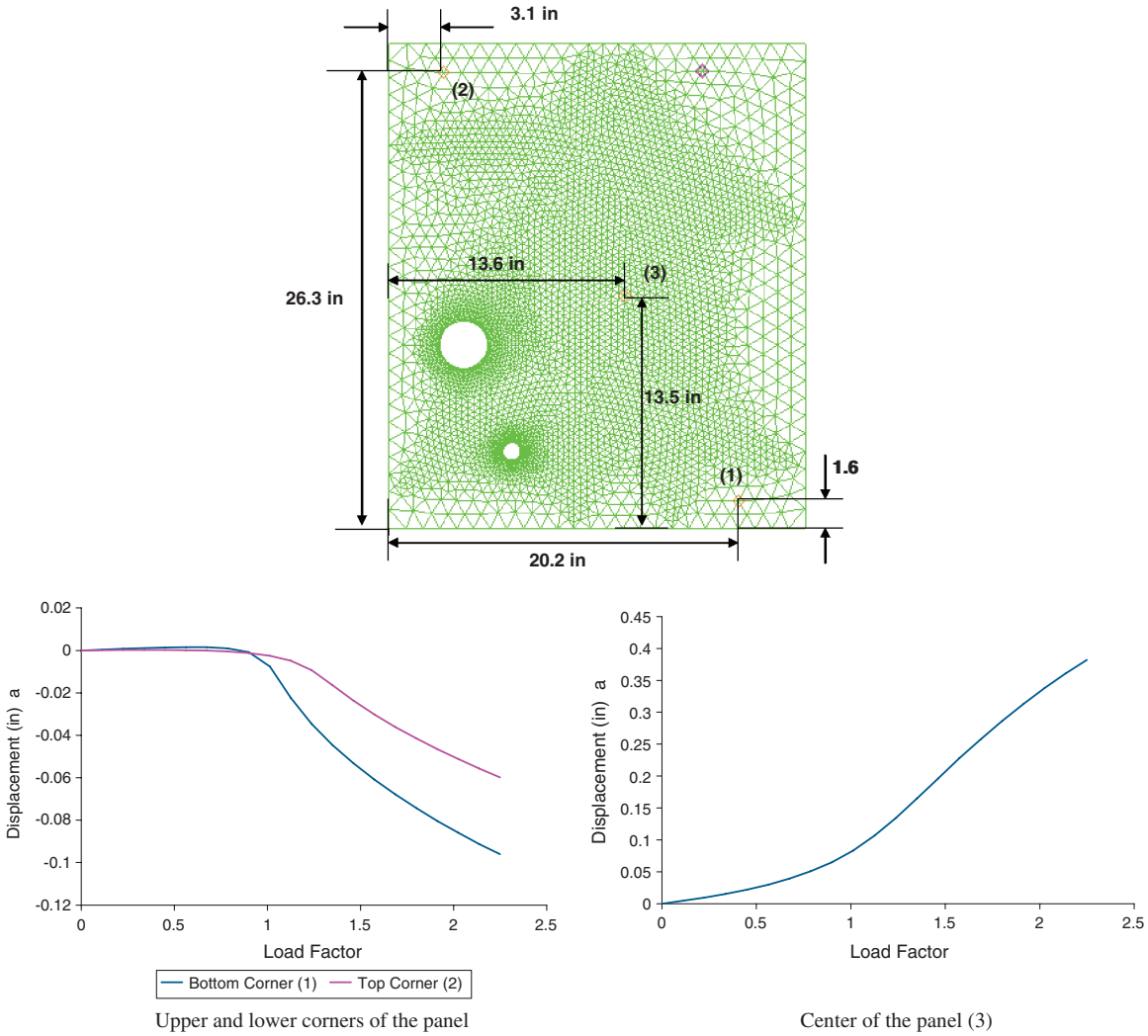

Fig. 23 Out-of-plane deflection at the upper and lower corners and the center of the panel versus load proportionality factor. Load proportionality factor normalized by the first buckling mode in the test fixture panel (load factor of 1.0 is 15.4 kips compression and 4.9 kips shear).

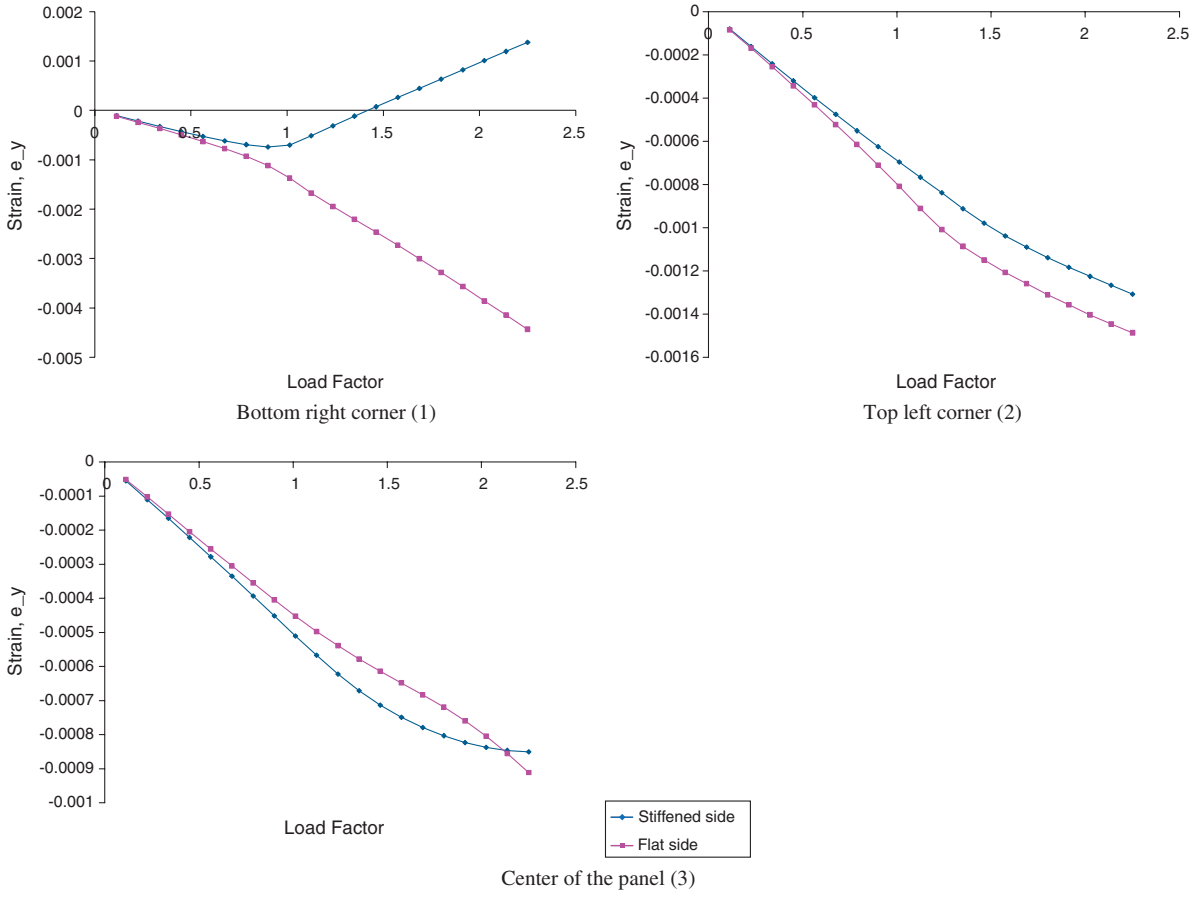

Fig. 24 Axial strain versus load factor for the bottom right, top left, and center of the panel.

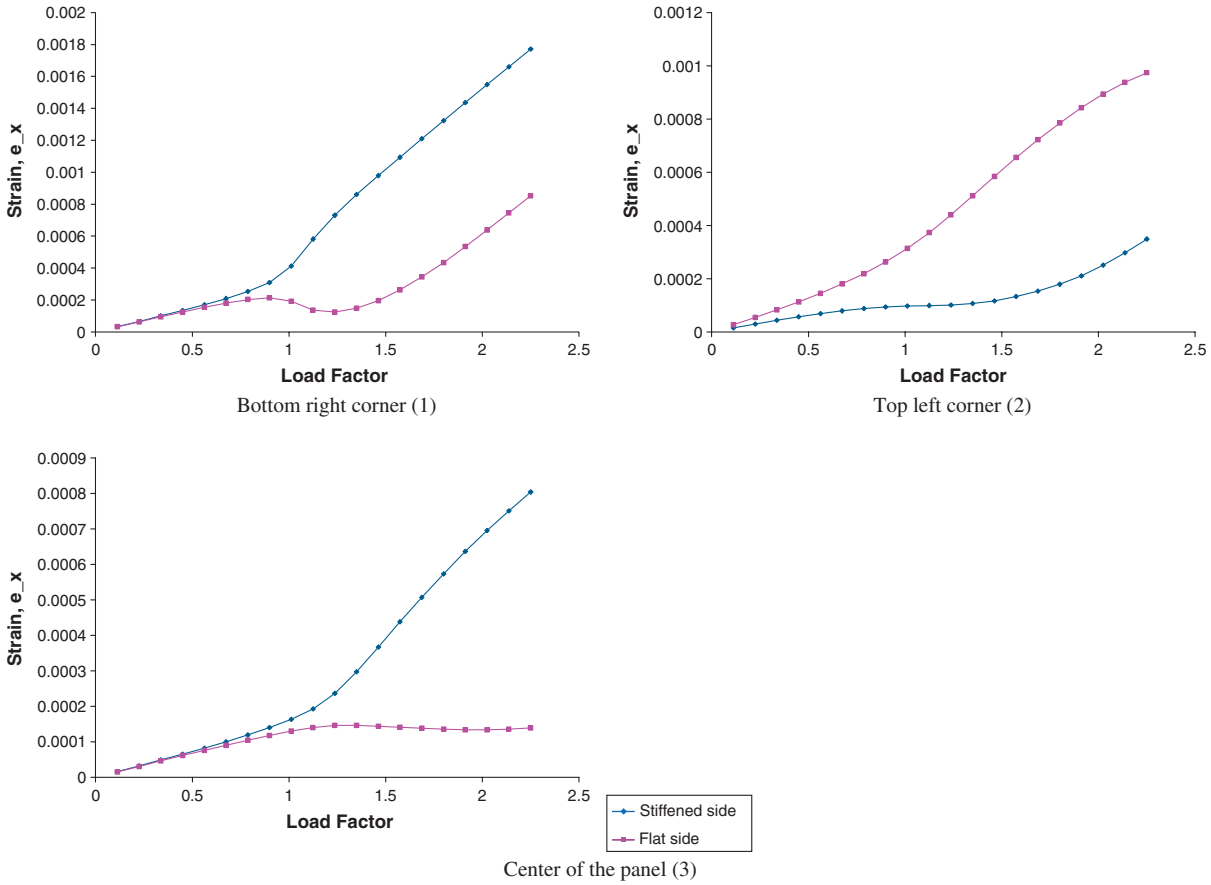

Fig. 25 Longitudinal strain component versus load factor for the bottom right, top left, and center of the panel.

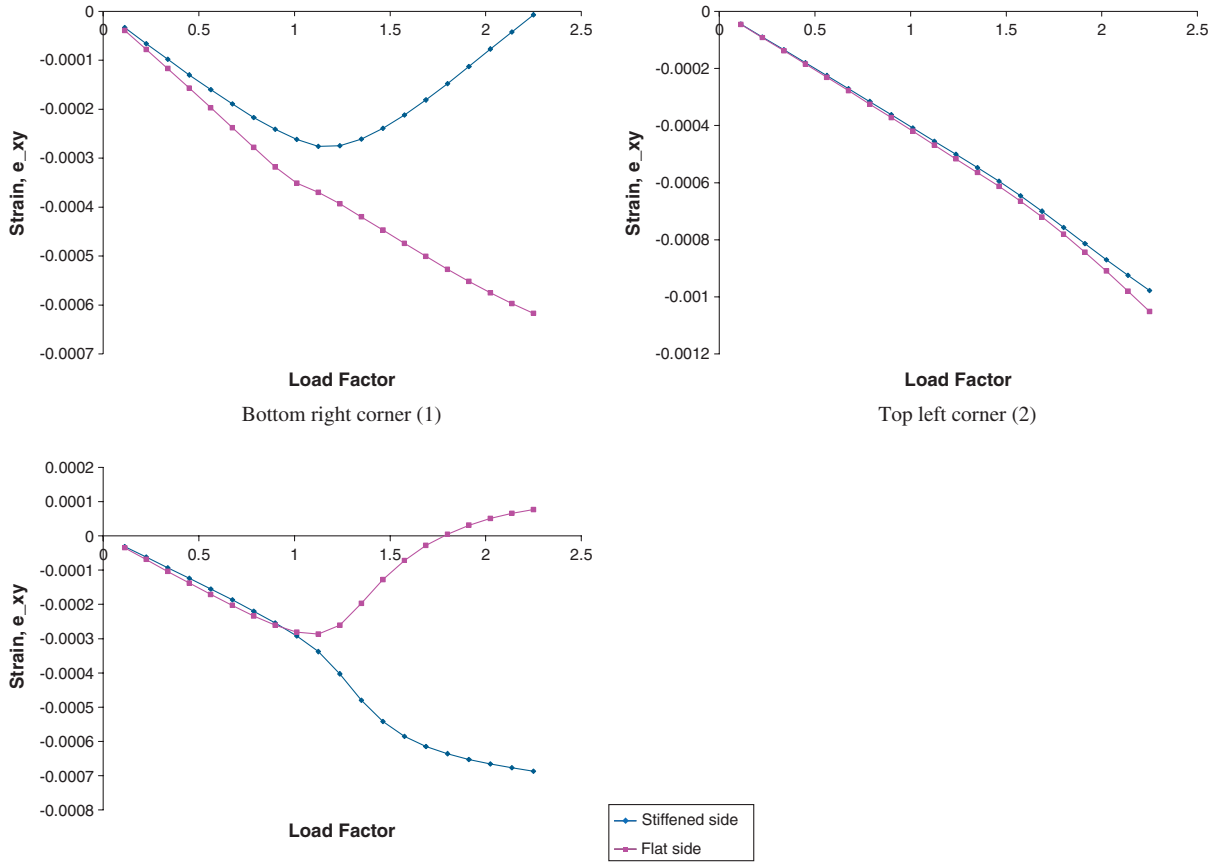

Fig. 26 Shear strain component versus load factor for the bottom right, top left, and center of the panel.

the compression dominated design load. The first three buckling mode shapes of the panel are shown in Fig. 22 below. Note that the initial buckle is predicted to occur in the lower right corner of the panel at a load 80% of the design load. The discrepancy between the design eigenvalue and that predicted in the test fixture model results from the difference between the ideal and actual boundary conditions and loading. Furthermore, the first mode shape seen in the test fixture is mode shape 5 of the response predicted by the ideal boundary conditions and loading (Fig. 19). Buckling mode 2 appears to be dominant at the top left corner of the panel. Buckling mode 3 represents the first global mode seen by the panel at approximately the design load level. During the experimental testing, it will be important to closely monitor the lower left and upper right corner of the panel using linear variable differential transformers and strain gages.

The nonlinear response of the panel for proportional compression-shear loading was examined until the onset of yielding. A simple bilinear stress strain curve for the Al 2139 was used. The yield stress was taken to be 64 ksi with a plastic stiffness of 5% of the elastic stiffness. The out-of-plane deflection and the in-plane strain components in the panel were taken at a point in the lower right corner of the panel, the center of the panel, and in the top left corner of the panel. The out-of-plane deflection of the panel was plotted against the load proportionality factor in Fig. 23. Note that the lower right corner experiences the initial buckle at the predicted eigenvalue, while the top left and center of the panel are predicted to buckle at higher load level. Moreover, at the edges, the buckle is severe with low post buckling stiffness; however, the center of the panel experiences a more smooth buckle.

Figure 23 shows out-of-plane deflection at the upper and lower corners and the center of the panel versus load proportionality factor. Load proportionality factor normalized by the first buckling mode in the test fixture panel (load factor of 1.0 is 15.4 kips compression and 4.9 kips shear).

The axial, longitudinal, and shear strain components on the flat and stiffened side of the panel was extracted from the three locations shown in Fig. 23 and were plotted against the load factor in Figs. 24–26, respectively. The results again illustrate that the buckling is quite severe at the bottom left corner. The FEM predictions will be used as the preliminary predictions for comparison in the experimentation.

At a load factor of 2.25, the finite element analysis indicated that substantial plastic deformation was occurring. Figure 27 indicates the location of the plastic deformation onset occurs at the stiffener–plate interface along the bottom edge of the panel. The accuracy of the predicted onset of plasticity in this location is questionable. The experimentally tested panel will include fillets at the base of the

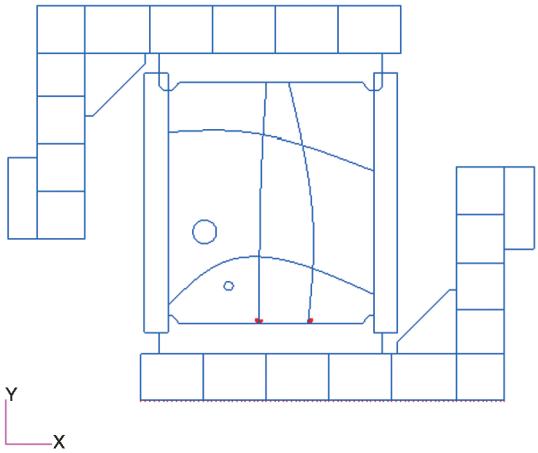

Fig. 27 Onset of yielding occurring at red areas at a load factor of 2.25 (34.65 kips compression and 11.0 kips shear).

stiffener which will act to dissipate the stress concentrations at these locations.

V. Conclusions

The paper presents a framework for the optimal design of complex unitized structures with multiple constraints under multiple-load cases. Multiple optimization studies of unitized structures with cutouts, straight stiffeners and curvilinear stiffeners are presented. The optimization is performed with an objective to minimize the structural mass with constraints on buckling, von Mises stress, damage tolerance, crippling and DaDT consideration. Panel thickness and stiffener sizes (height and thickness), stiffener orientations and curvatures along the size of rings around cutouts are used as design variables. Both uniform or nonuniform panel thickness are considered.

This framework couples the fracture, static stress and buckling analysis using ABAQUS with the external optimization software (VisualDoc) through the PYTHON scripting environment. The algorithms for the optimization problem such as the gradient-based optimization, the PSO, and the genetic algorithm are used for our optimization problem. The novel aspects of the current paper are: 1) damage tolerance analysis is included in the optimization process; 2) curvilinear stiffeners are used in optimal design; 3) optimization of stiffened panels with cutouts has been performed; and 4) ability to optimize over multiple-load cases simultaneously has been employed.

The current optimization procedure is illustrated with the help of realistic examples developed after consultations with industry partners. The results demonstrate the effectiveness of this framework, through a 7% weight reduction over the design that will result from the current design methodology of using only straight stiffeners. This design environment exploits the advantage of the availability of the finite element analysis software and the commercial optimizers, and has great potential for the design of aerospace stiffened structures.

A detailed nonlinear finite element analysis in MSC Nastran of the resulting design was performed in preparation for experimental testing at NASA Langley Research Center in the combined compression-shear test fixture. Out-of-plane deflection and strains at three locations on the panel were plotted against the load proportionality factor up until 2.25 times the buckling load at which point plastic deformation in the panel is predicted. The results presented herein provide substantial insight that will be critical during testing of the panel.

Acknowledgments

The work presented here was funded under NASA Subsonic Fixed Wing Hybrid Body Technologies NASA Research Announcements (NRA) (NASA NN L08AA02C) with Karen M. Brown Taminger as the application programming interface and the Contracting Officer's Technical Representative, and R. K. Bird as the Technical Monitor. We are thankful to all of them for their suggestions. The authors would also like to thank our partners in the NRA project, Robert J. Olliffe, Dave Havens, John Barnes, and Steve Englestad all of Lockheed Martin Aeronautics Company of Marietta, GA, for technical discussions. Finally, we express our sincere thanks to Sameer Mulani, Unitized Structure Group at Virginia Tech, for his useful insight.

References

[1] Pettit, R. G., Wang, J. J., and Toh, C., "Validated Feasibility Study of Integrally Stiffened Metallic Fuselage Panels for Reducing Manufacturing Costs," NASA CR-2000-209342, The Boeing Company, Long Beach, CA, May 2000.

[2] Nicholas, E. D., "Developments in the Friction-Stir Welding of Metals," ICAA Sixth International Conference on Aluminium Alloys, Toyohashi, Japan, 1998.

[3] Taminger, K. M. B., and Hafley, R. A., "Electron Beam Freeform Fabrication: A Rapid Metal Deposition Process," Proceedings of the Third Annual Automotive Composites Conference, Society of Plastics Engineers, Troy, MI, 9–10 Sept. 2003.

[4] Chan, K., Harter, J., Grandt, A. F., and Honeycutt, K., "Enhanced Crack Growth Methodology and Analyses for Unitized Structures," Ninth Joint FAA/DoD/NASA Conference on Aging Aircraft, Atlanta, GA, 6–9 March 2006.

[5] Renton, W. J., Olcott, D., Roeseler, W., Batzer, R., Baron, W., and Velicki, A., "Future of Flight Vehicle Structures (2000–2023)," *Journal of Aircraft*, Vol. 41, No. 5, 2004, pp. 986–997. doi:10.2514/1.4039

[6] Gurav, S. P., and Kapania, R. K., "Development of Framework for the Design Optimization of Unitized Structures," 50th AIAA/ASME/ASCE/AHS/ASC Structures, Structural Dynamics, and Materials Conference, AIAA Paper 2009-2186, Palm Springs, CA, 4–7 May 2009.

[7] Dang, T. D., Kapania, R. K., and Gurav, S. P., "Optimization of Unitized Structures Under Damage Tolerance Constraints," 50th AIAA/ASME/ASCE/AHS/ASC Structures, Structural Dynamics, and Materials Conference, AIAA Paper 2009-2550, Palm Springs, CA, 4–7 May 2009.

[8] Brighenti, R., "Buckling of Cracked Thin-Plates Under Tension Or Compression," *Thin-Walled Structures* Vol. 43, No. 2, 2005, pp. 209–24. doi:10.1016/j.tws.2004.07.006

[9] VISUALDOC Ver. 6.1., Vanderplaats Research and Development, Inc., 2008.

[10] Baker, D. J., "Combined Load Test Fixture," Army Research Lab., TM ARL-TR-3726, Hampton, VA, Feb. 2006.

[11] JSSG-2006, "Joint Service Specification Guide," Dept. of Defense, 1998.

[12] Kale, A. A., Haftka, R. T, and Sankar, B. V., "Efficient Reliability-Based Design and Inspection of Stiffened Panels Against Fatigue," *Journal of Aircraft*, Vol. 45, No. 1, 2008, pp. 86–97. doi:10.2514/1.22057

[13] Kreisselmeier, G., and Steinhauser, R., "Systematic Control Design by Optimizing a Vector Performance Index," *Proceedings of the IFAC Symposium on Computer-Aided Design of Control Systems*, Zurich, 1979, pp. 113–117.

[14] Collins, J. A., *Failure of Materials in Mechanical Design: Analysis, Prediction, Prevention*, Wiley, New York, 1993.

[15] Niu, M. C. Y., *Airframe Stress Analysis and Sizing*, 2nd ed., Conmilit, Hong Kong, 1997.

[16] Bird, R. K., Taminger, K. M. B., Slemp, W. C. H., and Kapania, R. K., "Design, Optimization and Evaluation of Integrally-Stiffened Al-7050 Panel with Curved Stiffeners," NASA TR, 2010 (to be published).